CrossMark

Effect of electrodepositing Ag on DC etching aluminum foils for electrolytic capacitor

C. L. Ban[1,2] · S. Q. Zhu[3] · J. L. Hou[2] · F. R. Wang[1] · J. Wang[1]

Abstract Ag nuclei were electrodeposited on the surface of aluminum foil to induce tunnel etching. The effects of Ag nuclei on the surface and cross-section etching morphologies and electrochemical behavior of Al foil was investigated with SEM, polarization curve (PC) and electrochemical impedance spectroscopy (EIS). It is proved that the tunnels etched in this way are distributed more uniformly and the density of tunnels and pits are enhanced, leading to increase in specific capacitance of etched Al foil. These effects can be attributed to the mechanism that the Ag nuclei can serve as the favorable sites for tunnel initiation on aluminum foil surface owing to the formation of Ag–Al micro-batteries, in which Ag is cathode and Al is anode. This mechanism is supported by the SEM, PC and EIS.

1 Introduction

Aluminum electrolytic capacitors which have high specific capacitance, small size, and self-healing properties are widely used in devices such as computers, mobile phones, and vehicles. The electric capacitance (C) of Al electrolytic capacitors can be expressed by the following formula, $C = (\varepsilon_o \varepsilon_r S)/d$, where ε_o is the vacuum dielectric constant, ε_r is the relative dielectric constant of the Al anodic oxide film, S is the specific internal surface area of Al foil electrode, and d is the film thickness. The enlargement of S is performed by electrochemical etching high-purity Al foils with {001} in strong acid solutions, using crystallographical dissolution. The increase in ε_r and reduction in d is achieved by anodizing etched foil in weak acid solution when the formation voltage is fixed [1–3]. Recently, it is popular to form high ε_r composite oxide films such as Al_2O_3-(TiO_2, $BaTiO_3$, ZrO_2, Ta_2O_5, Nb_2O_5, etc) by electrodeposition, hydrolysis precipitation, sol–gel coating and anodizing [4–8]. However, the industrial application of such composite films is unfavorable due to their high dielectric loss and leakage current. The electrochemical etching is still the most important practical way to increase C.

Many variables are involved in the DC-etching process, including the grain size, cubicity and impurities or pre-existing flaws of pure Al foil, pretreatments, acid composition, concentration and temperature, and current parameters [9–13]. As a popular technique used in industry, some cathodic trace elements, such as Pb, Sn, or Bi, were added into the crude aluminum and then concentrated at the oxide–metal interface of aluminum foils by the driving of heat treatment so as to induce the tunnel etching of aluminum foils by galvanic corrosion effect. The concentrated trace elements, however, are not randomly and uniformly distributed at the oxide-metal interface of aluminum foils but favorably segregated at lattice defects such as dislocations, grain boundaries, and vacancies, etc. These concentrated elements will result in serious merging of etch tunnels and reduction of the foil thickness and effective area after etching [14–17].

Recently, much attention has been actively focused on controlling the nucleation and growth of tunnels etched on aluminum foil more precisely [18, 19]. For example, a

✉ C. L. Ban
    banchaolei@163.com

1   School of Materials Science and Engineering, Liaocheng University, Liaocheng 252059, China

2   Mechanical and Electronic Engineering College, Shandong Agricultural University, Tai'an 271018, China

3   School of Computer Science, Liaocheng University, Liaocheng 252059, China

physical mask film with an ordered array of holes was prepared on the surface of aluminum foil to control the tunnel initiation accurately [20]. Electro-less plating Pb, In or Zn on the surface of aluminum foil could induce tunnel etching of aluminum foil effectively. But, the physical mask film can be hardly applied in the large-scale production. The electro-less plated inert elements are very rich and concentrated easily along the rolling lines and the merging of the etch tunnels on aluminum foil surface is still very serious [15, 21, 22]. In order to dissolve the above problems, new methods are called for. In this work, the Ag nuclei have been electrodeposited on the aluminum foil surface to induce the tunnel initiation of aluminum foil in large scale. The effects of such Ag nuclei on the tunnel etching behavior of aluminum foil have been investigated in detail.

2 Experimental

2.1 Electrodepositing Ag nuclei and DC-etching

The specimen in this experiment is commercial aluminum foils for high voltage electrolytic capacitors, with 99.99% purity, 95% (100) cubicity and 110 μm thickness. The foils were cut into a rectangular shape with dimension of 13 cm×6 cm and then mounted into a polypropylene holder having an exposed area of 9 cm×5 cm for electrodepositing or etching. Two graphite electrode plates of 15.5 cm×6.5 cm×8 cm size were used as counter electrodes, with a gap of 25 mm between them. The specimen was placed parallel to the two electrode plates with a distance of 10 mm between each of them. Temperature of the solution was measured by alcohol thermometer and controlled by heating blender and temperature controller.

Electrodepositing Ag nuclei on Al foil surface was carried out in 0.05 M $AgNO_3$ solutions at room temperature for different time. The applied current density was 10 mA cm^{-2}. Before electrodepositing, these specimens were immersed in 0.125 mol/L NaOH at 40 °C for 30 s to remove the surface oil contaminaton and activate the surface.

The aluminum foils were DC-etched by two steps: tunnel formation and tunnel widening. In the tunnel formation, a current density of 200 mA cm^{-2} was applied to the aluminum foils in a mixed solution of 1N HCl + 5N H_2SO_4 solution at 85 °C for 100 s. Subsequently, in the tunnel widening step, the aluminum foils were etched at a current density of 50 mA cm^{-2} in 3 wt.% HNO_3 solution at 70 °C for 700 s.

The DC-etched foil was anodized at 90 °C in 150 g/L $C_6H_{16}N_2O_4$ for producing the anodic oxide film as dielectric layer by applying 100 V for 10 min and the special

capacitance of the film was measured with a LCR meter in 150 g/L $C_6H_{16}N_2O_4$ at 30 °C.

Some specimens were only rinsed with deionized water as comparative blank examples. All solution used in this work was prepared from reagent grade chemicals and deionized water. Between any two steps, specimens were thoroughly and completely rinsed with deionized water.

2.2 Surface and cross-section morphology observation

After electrochemical etching, the samples were rinsed thoroughly with deionized water and dried in ambient condition. For surface morphology studies, the sample was examined under a scanning electron microscope (SEM, LEO 435VP). For sectional observation, which would shed light on tunnel development, the etched samples were anodized, mounted vertically in epoxy resin, mechanically polished, chemically dissolved in iodine methanol solution (10% I_2/CH_3OH), sputter-coated with gold and examined under SEM. The pit density and size distribution were determined from the analysis of the SEM images, each covering 127×86 μm. All the analysis was conducted by the Image-Pro Plus software.

2.3 Electrochemical property measurement

The polarization curves and EIS was measured to investigate the electrodepositing Ag nuclei on the DC etching aluminum foils. The electrochemical cell was consisted of three electrodes and solution. The specimens of aluminum foils with an exposure area of 1 cm^2 to the solution, Pt foil and Ag/AgCl/sat. KCl electrode were used as the working electrode (WE), counter electrode (CE) and reference electrode (RE) respectively. The solution composition and temperature was the same with DC-etching. The electrochemical measurements were carried out by the multichannel potentiostats (CHI660). The PC measurements were carried out with a sweep rate of 10 mV/s. The EIS spectra were obtained over the frequency range of 10 mHz to 100 kHz with an applied AC perturbation potential of 10 mV amplitude. The experimental results were interpreted on the basis of an equivalent circuit determined using a suitable fitting procedure described in Zsimpwin software.

3 Results and discussion

3.1 Effect of electrodepositing Ag on surface morphologies of etched foil

Figure 1 shows the SEM surface images of etched Al foil without electrodepositing (blank) and with electrodepositing Ag for different time (b, c, d), respectively, and in insets

Fig. 1 Surface morphologies of conventional etched Al foil (**a**) and different time electrodepositing Ag-assisted ones **b** 5 s, **c** 10 s, **d** 15 s
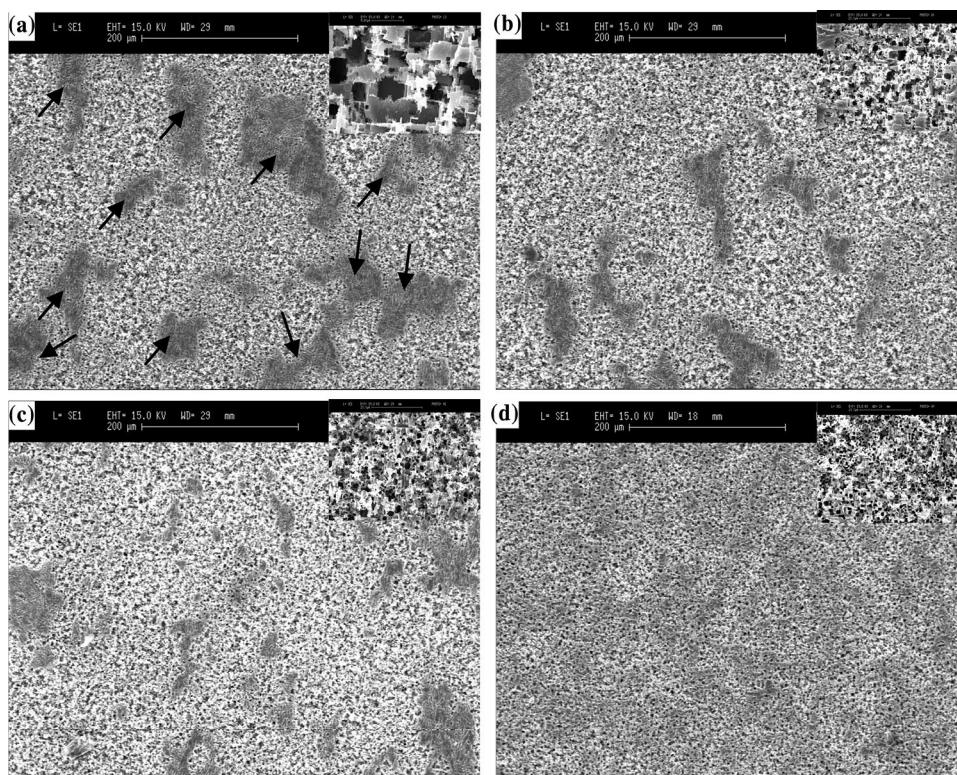
magnified morphologies. It is found that there are noticeable differences in the morphologies of etch pits, depending on the electrodepositing Ag. For the conventional blank specimen, the etched foil displayed quite uneven topography with dispersed intact or slightly corroded aluminum zones, as shown by black arrows in Fig. 1a. However, with imposition of electrodepositing Ag, these areas tend to disappear, replaced by a uniform etched topography, just shown by Fig. 1b, c, d. Moreover, when the time for electrodepositing Ag is increasing, the tunnel density increases greatly and the tunnel distribution becomes more homogeneous, as shown in Fig. 1d. Meanwhile, the insets magnified morphologies further demonstrate that a high density of narrow pits was induced by ultrasound irradiation and the average pit size simultaneously decreased because the high density of pits had to supply the same amount of applied charge.

3.2 Effect of electrodepositing Ag on cross-section morphologies of etched foil

Figure 2a–d shows the etch pit cross-section distribution formed by the conventional DC etching and different time electrodepositing Ag-assisted ones, respectively. The shape and array of etch tunnels developed along ⟨100⟩ directions are observed in Fig. 2. It clearly shows the effect of electrodepositing Ag on the tunnel shape, size, density and distribution. The tunnels for blank sample are generally sparse in distribution and coarse in size. With imposition of electrodepositing Ag and increasing its time, the tunnels become dense and uniform in distribution and fine in size, in consistent with observation from Fig. 1.

During electroplating Ag before etching, Ag^+ in the solution was electro-migrated to the Al foil, adsorbed electrons, reduced to Ag atoms and deposited on the surface of Al foil. These Ag atoms constitute Al–Ag local micro galvanic cells, in which Ag acts as cathode and Ag acts as anode. When electroplating was extended, more Al–Ag micro galvanic cells will formed on the Al foil surface. These micro galvanic cells will cause Al substrate to suffer from severe corrosion, leading to increase in pits and tunnels density, as shown by Figs. 1 and 2. The deposited Ag is maybe randomly distributed rather than preferentially one. The pitting resistance for those intact or slightly corroded aluminum zones, as shown by black arrows in Fig. 1a decreased by these randomly distributed micro galvanic cells, leading to improvement in tunnels and pits distribution.

3.3 Effect of electrodepositing Ag on electrochemical property of Al foil during DC-etching

Figure 3a shows the polarization curves in etching solution for blank sample and different time electrodepositing Ag-assisted ones in etching solution. It can be fond that the pitting current, i_p, for blank sample are the most negative.

Fig. 2 Cross section morphologies of conventional etched Al foil (**a**) and different time electrodepositing Ag-assisted ones **b** 5 s, **c** 10 s, **d** 15 s
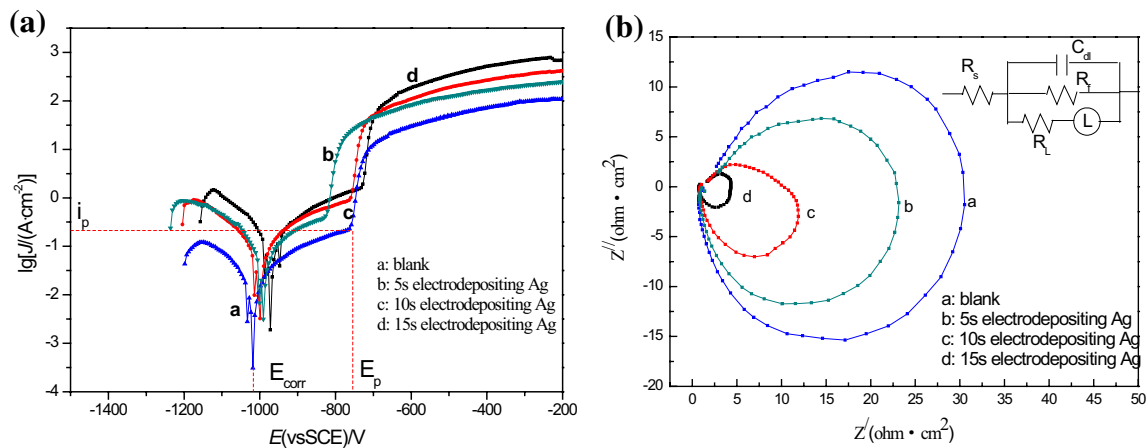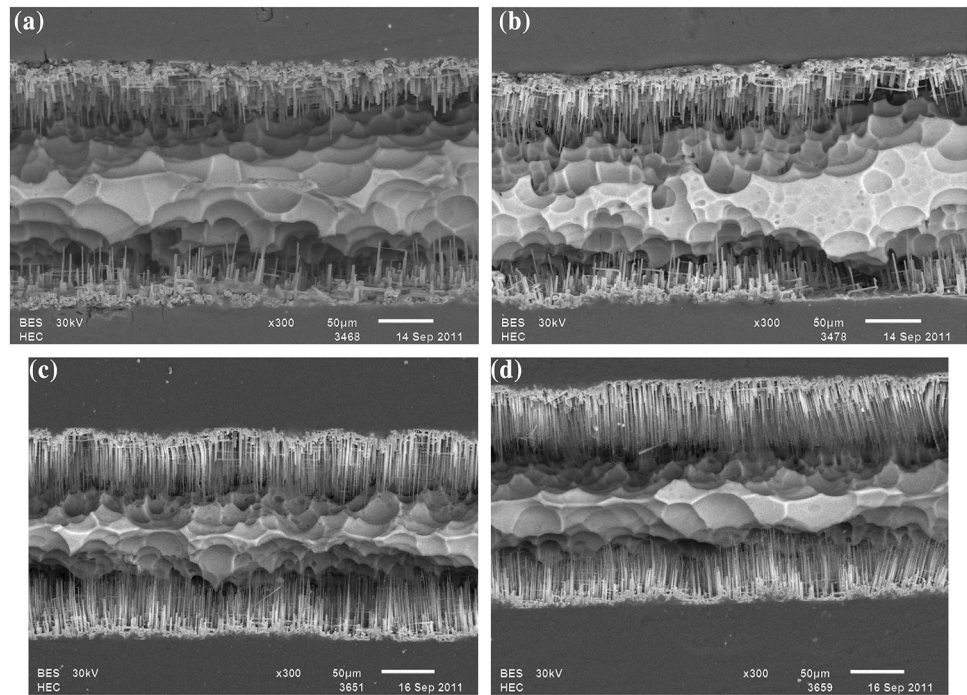

Fig. 3 Effect of electrodepositing Ag on electrochemical properties of Al foil during DC-etching **a** polarization curves; **b** electrochemical impedance spectra

With introduction of ectrodepositing Ag and increasing its time, the i_p gradually shift toward to a more positive value. Meanwhile, the pitting potential, E_p, for all the samples was nearly equal, apart from sample b the E_p for which decreased. These facts suggest that the Al foil surface will surer from severe pitting during the DC etching due to formation of Al-Ag micro-galvanic cells, in consistent with Figs. 1 and 2. However, the corrosion potential, E_{corr}, has a slow tendency of increase with introduction of ectrodepositing Ag and increasing its time. It is well known that the equilibrium electrode potential value of Ag is much larger than that of Al. With introduction of ectrodepositing Ag

and increasing its time, more Ag atoms will deposit on the Al foil surface or replace the Al atoms in the lattice, leading to positive shift in E_{corr}. The E_{corr}, E_p and i_p for different samples are listed in Table 1.

Figure 3b shows the effect of ectrodepositing Ag on electrochemical impedance spectra of Al foil, in which the measured impedance spectra are plotted into Nyquist diagram. It is clearly seen that the Nyuist diagram is mainly composed of a capacitive arc at high frequency and an inductive loop at low frequency. CAO et al. [16] thought that the appearance of inductive component is the important feature of EIS during pit incubation and the inductive

Table 1 The circuit parameters from the EIS data and special capacitance (C_{100}) of 100 V formation voltage

	E_{corr} (mV, vsSCE)	E_p (mV, vsSCE)	i_p (A·cm^{-2})	C_{dl} (μF·cm^{-2})	R_f (Ω·cm^{-2})	C_{100} (μF·cm^{-2})
Blank	−1015	−755	0.2186	6.190	29.11	2.011
5 s electrodepositing Ag	−993	−819	0.4132	7.738	22.54	2.442
10 s electrodepositing Ag	−1001	−740	0.9181	11.48	11.62	2.951
15 s electrodepositing Ag	−972	−730	1.5448	12.01	4.76	3.184

arc is linked to the passive film on the surface. KEDDAM et al. [17] thought that the inductive loop observed is associated with the weakening of the protective effectiveness of the aluminum oxide layer due to the anodic dissolution of aluminum alloy. But the physical meaning of negative resistance and negative capacitance is not definite. The high-frequency impedance arc is generally attributed to the processes occurring at the electrode–electrolyte interface, indicating the ion transfer resistance and the capacitance of electric double layer at the electrode–electrolyte interface.

The EIS can be further analyzed by fitting the equivalent circuit model in the inserted figure of Fig. 3b, where C_{dl} is double layer capacitance and proportional to the specific surface area of the etched area, R_f is charge transfer resistance, R_s is the solution resistance, R_L and L are equivalent resistance and inductance, respectively. Table 1 lists the parameters from the equivalent circuit model, in which the C_{dl}, R_f, R_s and special capacitance (C_{100}) of 100 V formation voltage anodic oxide film are also listed. The physical meanings of R_L and L are vague, and their values are not given here. As shown in Table 1, with ectrodepositing Ag and prolong its time, the C_{dl} and C_{100} gradually increase and R_f gradually decreases, which can be accounted for by formation of more Ag–Al micro galvanic local cells, serving as primary sits for pitting and leading to enhancement in i_p and more pits and tunnels, in consistent with Figs. 1, 2, and 3a.

4 Conclusions

In the present study, the Ag nuclei have been electrodeposited on the surface of aluminum foil by fast electrodeposition in Ag$^+$-containing solution. The effect of electrodeposited Ag nuclei on the tunnel etching behavior of aluminum foil has been elaborately investigated and some conclusions can be summarized as follows. Electrodepositing Ag can form micro Ag–Al galvanic local cells on the Al foil surface, which make Al foil more vulnerable to pitting so as to increase the density of pits and tunnels during DC-etching, enlarge the special area of etched foil, enhance its special capacitance and improve the uniformity of pits and tunnels distribution of etched Al foil.

References

1. C.L. Ban, Y.D. He, X. Shao, J. Mater. Sci. Mater. Electron. **24**, 3442 (2013)
2. C.L. Ban, Y.D. He, X. Shao, L.P. Wang, J. Mater. Sci. Mater. Electron. **25**, 128 (2014)
3. S.Q. Zhu, C.L. Ban, L.J. Jiang, J. Mater. Sci. Mater. Electron. **26**, 5703 (2015)
4. Z.S. Feng, J.J. Chen, R. Zhang, N. Zhao, Ceram. Int. **38**, 3057 (2012)
5. L. Xiang, S.S. Park, Appl. Surf. Sci. **388**, 245 (2016)
6. X.F. Du, Y.L. Xu, J. Sol-Gel. Sci. Technol. **45**, 57 (2008)
7. S.S. Park, B.T. Lee, J. Electroceram. **13**, 111 (2008)
8. C.L. Ban, J.L. Hou, S.Q. Zhu, C.Z. Wang, J. Mater. Sci. Mater. Electron. **27**, 1547 (2016)
9. C.L. Ban, Y.D. He, X. Shao, Corros. Sci **78**, 7 (2014)
10. C.L. Ban, Y.D. He, X. Shao, J. Du, Trans. Nonferr. Met. Soc. China **23**, 1039 (2013)
11. C.L. Ban, Y.D. He, Trans. Nonferr. Met. Soc. China **19**, 601 (2009)
12. C.L. Ban, S.Q. Zhu, X.Q. Tao, W.Y. Chen, J. Mater. Sci. Mater. Electron. **27**, 12074 (2016)
13. Y.H. Chiu, B.L. Ou, Y.L. Lee, Korean J. Chem. Eng. **24**, 881 (2007)
14. Z. Ashitaka, G.E. Thompson, P. Skeldon, G.C. Wood, K. Shimizu, J. Electrochem. Soc. **146**, 1380 (1999)
15. W. Lin, G.C. Tu, Y.M. Peng, Corros. Sci. **38**, 889 (1996)
16. J. Tan, J.C. Walmsley, B. Holme, H. Nordmark, K. Nisancioglu, Corros. Sci. **68**, 204 (2013)
17. K. Arai, T. Suzuki, T. Atsumi, J. Electrochem. Soc. **132**, 1667 (1985)
18. S.Q. Zhu, C.L. Ban, X.Q. Tao, W.Y. Chen, L.J. Jiang, J. Mater. Sci. Mater. Electron. **26**, 6750 (2015)
19. N. Peng, Y.D. He, H.Z. Song, X.F. Yang, X.Y. Cai, Corros. Sci. **91**, 2013 (2015)
20. T. Fukushima, A. Takeda, K. Nishio, H. Masuda, Electrochem. Solid State **13**, C17 (2010)
21. W. Lin, G.C. Tu, C.F. Lin, Y.M. Peng, Corros. Sci. **39**, 1531 (1997)
22. C.L. Ban, Y.D. He, X. Shao, J. Du, L.P. Wang, Trans. Nonferr. Met. Soc. China **23**, 3650 (2013)